

A Finite Element Model of the Pelvis and Lower Limb for Automotive Impact Applications

Costin D. Untaroiu¹, Jaeho Shin², Neng Yue²,
Young-Ho Kim³, Jong-Eun Kim³, Alan W. Eberhardt³

¹Virginia Tech, Blacksburg, VA, USA

²University of Virginia, Charlottesville, VA, USA

³University of Alabama at Birmingham, Birmingham, AL, USA

Abstract

A finite element (FE) model of the pelvis and lower limb was developed to improve understanding of injury mechanisms of the lower extremities during vehicle collisions and to aid in the design of injury countermeasures. The FE model was developed based on the reconstructed geometry of a male volunteer close to the anthropometry of a 50th percentile male and a commercial anatomical database. The model has more than 625,000 elements included in 285 distinct components (parts). The material and structural properties were selected based on a synthesis of current knowledge of the constitutive models for each tissue. The model was validated in seventeen loading conditions observed in frontal and side impact vehicle collisions. These validations include combined axial compression and bending (mid-shaft femur, distal third leg), compression/flexion/xversion/axial rotation (foot), and lateral loading (pelvis). In addition to very good predictions in terms of biomechanical response and injuries, the model showed stability at different severe loading conditions. Overall results obtained in the validation indicated improved biofidelity relative to previous FE models. The model may be used in future for improving the current injury criteria of lower extremity and anthropometric test devices. Furthermore, the present pelvis and lower limb was coupled together with other body region FE models into the state-of-art human FE model to be used in the field of automotive safety.

Introduction

Occupant pelvis-lower extremity (PLEX) injuries in automotive crashes account for 26% of AIS 2+ injuries for belted passengers (Morgan et al. 1990). 55% of these injuries occur in the Knee-Thigh-Hip (KTH) complex and account for 42% of the life-years lost to injury for occupants in airbag equipped vehicles (Kuppa et al. 2001). To develop a better understanding of Crash-Induced Injuries (CIIs) required in designing injury countermeasures, several experimental and numerical approaches have been used (Crandall et al. 2011). Experimental approaches have been tried to replicate CIIs in lab conditions using Post Mortem Human Subjects (PMHS) impact tests. However, understanding the injury mechanisms and development of accurate Injury Criteria using this test data is challenging due to inherent variations in terms of PMHS anthropometry and material properties. With recent rapid increases in computational power, several human numerical models have been used for vehicle safety research and development. The human finite element (FE) models are currently the most sophisticated human numerical

models, which can provide general kinematics of the whole human body model and calculate the detailed stress/strain distributions which can be correlated with the risk of injuries.

While several FE PLEX models have been developed to investigate traffic accidents involving occupants in vehicles and pedestrians, limitations arise from their geometries, the modeling approaches used to represent their components, and limited test data used for model validation. In some models, the whole lower limb geometry or some of their components were obtained by uniformly scaling the geometry of the Visible Human dataset (Silvestri et al. 2009, Kim et al. 2005). This approach introduced inherently some local inaccuracies of the model. In other models (e.g. Huang et al. 2001, Beillas et al. 2001, Silvestri et al. 2009), the geometry of ligaments and thicker layers of cortical bone were simplified by modeling those components as bar and shell elements, respectively. Finally, all previous models could not benefit from the huge amount of material and component test data published recently.

The objective of this study was to develop a more biofidelic occupant PLEX FE model using the geometry directly reconstructed from the medical scan data of a 50th percentile male volunteer.

Methods

Model Development

The geometry reconstruction of the occupant LEX was conducted by the Center for Injury Biomechanics, Virginia Tech-Wake Forest University (Gayzik et al. 2011). A male volunteer with anthropometric characteristics (175.3 cm height and 77.1 kg weight) close to the 50th percentile male (175.3 cm/78.2 kg - Hybrid III dummy, 175.8 cm/78 kg - Gordon et al. 1988) was recruited to develop an extensive image data set. The resolution/ thickness of the computed tomography (CT) and magnetic resonance imaging (MRI) scans were 0.98/ 1.25 mm and 1.5/ 1.6 mm, respectively. The geometries of the bony structures and soft tissues of the volunteer PLEX region were reconstructed using the CT and MRI scanned images, respectively. Since the segmentation accuracy depends on the CT scanner characteristics, the limit threshold for thickness was set as a 2.75 mm based on the field of view (FOV) used in acquiring the CT scans (Gayzik et al. 2011). Thus, the regions with cortical thickness under this value (e.g. pelvic bone, epiphysis regions, etc.) were prescribed by offsetting the exterior surface by appropriate values reported in the literature.

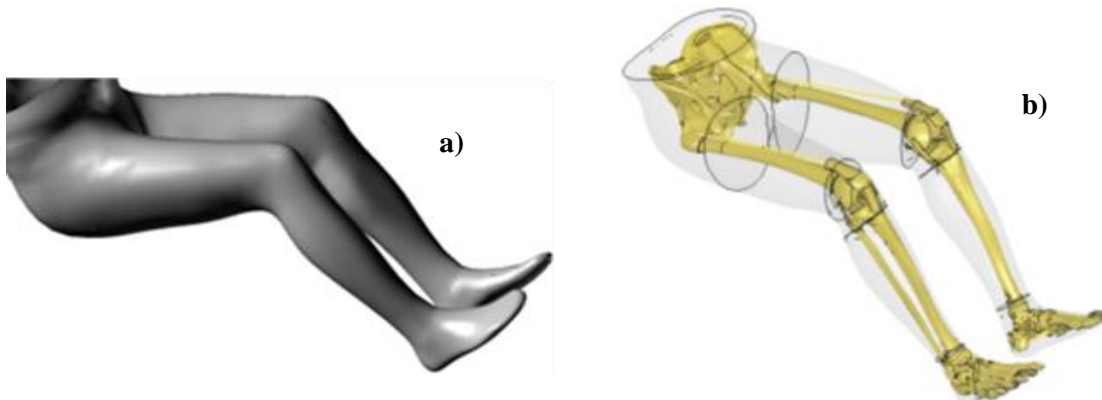


Figure 1. PLEX a) model geometry b) model mesh (flesh is transparent)

For example, the pelvic cortical bone was modeled by hexahedral elements with the thickness assigned based on the pelvis model reported by Anderson et al. (2005). The transfer of thickness from the Anderson model to the present pelvis model was performed using shape-preserving parameterization and mesh moving techniques (Kim et al., 2012). The geometric data of foot ligaments and tendons were determined according to a commercial database of human geometry (<http://www.3dcadbrowser.com>). The knee flexion angle of the scanned LEX was about 120° to mimic the seating posture of the occupant LEX in a vehicle (Robbins et al. 1983).

Two meshing approaches, structural and unstructural, were employed to achieve a good mesh quality. The structural mesh technique consists of filling the solid object with cubic blocks (the mesh topology) and projecting the outer and inner boundaries to the exterior and interior surfaces of the object. Structural IA-FEMesh (University of Iowa, Iowa City, IA), TrueGrid (XYZ Scientific Applications, Livermore, CA) and HyperMesh 10 (Altair HyperWorks, Troy, MI) were used to mesh the coxal bone, sacrum, tibia, fibula, knee ligaments (anterior cruciate ligament (ACL), posterior cruciate ligament (PCL), medial collateral ligament (MCL) and lateral collateral ligament (LCL)), knee tendons (femoral and tibial), menisci (medial and lateral) and flesh. The cortical bones in the diaphysis regions of the tibia and fibula were meshed using HyperMesh 10 and the trabecular bones in the epiphysis regions of those long bones were meshed by IA-FEMesh.

Material models included in the library of the explicit and implicit LS-DYNA 971R4 solver (LSTC, Livermore, CA) were assigned to all lower limb parts. The cortical and trabecular bones were modeled as an isotropic elastic-plastic material and have similar mechanical properties in tension and compression loading, due to the lack of more complex material models for bone in the LS-DYNA material library. Cortical bone fracture was modeled by the element elimination method, with a fracture threshold of 0.88 % effective plastic strain (Untaroiu 2005). While the same material properties were assigned in the diaphysis region of the long bones, the cortical bone is softer toward the bone ends within the epiphysis according to literature data. Therefore, different material properties were assigned to the femoral head sub-chondral bone (Yue et al. 2011).

A quasi-linear viscoelastic (QLV) material model (MAT_92, LS-DYNA manual) was assigned to the knee ligaments to provide transversely isotropic material symmetry with high stiffness along the fibers (parallel to the normal of the assigned hexahedral element) in tension, and negligible stiffness in compression or along directions included in the transverse plane. Knee ligament rupture threshold was defined as the maximum principal strain of 0.4 (Takahashi et al. 2000). The flesh was defined as a simplified rubber/foam model with the dynamic engineering compressive stress-strain curve defined by Untaroiu (2005) and tensile stress-strain curve defined by Yamada (1970). The elastic modulus of the hip joint ligaments was assigned as 0.15 GPa which is in the range value reported by Hewitt et al. (2001) (0.076 - 0.286 GPa). The rest of the soft tissue material models and their initial parameters were assigned accordingly based on a previous pedestrian LEX FE model (Untaroiu 2005).

While a full integration scheme was used for shell elements, one point integration scheme with constant stress was used for solid elements. The LS-DYNA hourglass types of standard viscous form and Flanagan-Belytschko stiffness form with exact volume integration were used for soft tissues and bony structures, respectively. After the left lower limb FE model was developed, the corresponding right lower limb was created by reflection along the middle sagittal plane of the specimen, and then both limbs were connected with the pelvis model.

Model Validation

To check the predictability of the PLEX model for the Crash Induced Injuries (CIIs), 17 impact validations corresponding to frontal and lateral loading (Fig. 2) were conducted (Table 1-2).

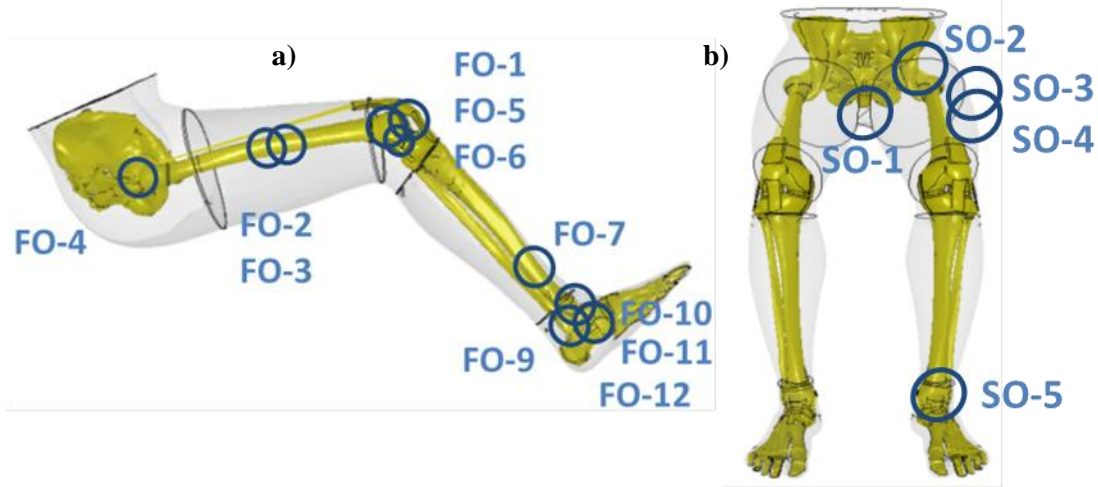


Figure 2. Model Validation for a) frontal loading and b) lateral loading

Table 1. The list of model validations of PLEX model under frontal impact loading.

Validation ID	CII	Main Loading	Validation Studies
FO-1	Hip	Compressive	Rupp et al. (2002, 2003)
FO-2	Mid-shaft Femur	Bending, Combined (Compression, Bending)	Funk et al. (2004)
FO-3			Ivarsson et al. (2009)
FO-4	Proximal Femur	Compression	Keyak et al. (1998)
FO-5	Proximal Femur	Compression	Rupp et al. (2003)
FO-6	Knee	AP Shear, Compression	Balasubramanian et al. (2004)
FO-7	Mid-shaft Leg	Combined (Compression, Bending)	Untaroiu et al. (2008)
FO-8	Ankle and Subtalar Joint	Compression, Flexion, Xversion, Internal and External Rotation	Chen et al. (1988)
FO-9			Funk et al. (2002)
FO-10			Funk et al. (2000)
FO-11			Rudd et al. (2004)
FO-12	Hindfoot (calcaneus)	Compression	Funk et al. (2000)

Table 2. The list of model validations of PLEX model under side impact loading (SO).

Validation ID	CII	Main Loading	Validation Studies
SO-1	Pelvis	Lateral Compression	Dakin et al. (2001)
SO-2			Guillemot et al. (1997, 1998)
SO-3			Beason et al. (2003)
SO-4	Lateral Bending	Lateral Bending	Keyak et al. (1998)
SO-5	Xversion	Xversion	Funk et al. (2002)

The FE models of test set ups were developed and then were connected with the PLEX models to accurately replicate boundary conditions corresponding to PMHS component tests. The input data in the component validations was usually defined as the time histories of impactors recorded in testing. The time histories of impact loading and the injuries predicted by the models were recorded and compared with PMHS test data.

Stability Check of the FE Model under Severe Impact Loading Condition

After performing all component validations (Tables 1-2), the stability of whole PLEX model under four severe loading conditions corresponding to traffic accidents was also verified. In the first simulation (Fig. 3a), an initial velocity of 4.9 m/s was assigned to the whole PLEX model toward a fixed rigid plate to simulate the impact between the knee and the knee bolster. The motion of the pelvis bone was set free only along the impact direction, and the impact was successfully simulated up to 100 ms. The footwell intrusion typically seen in frontal impacts was simulated by the normal impact between a 25 kg rigid impactor model with a padding layer and the feet models (Fig. 3b). The pelvis bone region of PLEX model was fixed and a 5.6 m/s initial velocity was assigned to the impactor as in Kuppa et al. (1998).

Two other impact simulations were performed in impact conditions corresponding to side impact accidents. To simulate the vehicle door intrusion to the occupant lower extremity, an initial velocity of 6.9 m/s was assigned to a rigid plate towards the knee region of the whole PLEX model (Fig. 3 c). In this simulation, the motion of the pelvis bone was constrained in all six degree of freedom. Finally, the PLEX model was impacted laterally by a rigid impactor similar to that used by Bouquet et al. (1998). In order to replicate the experimental dynamic tests, a rigid wall for the seat and a linear impactor (200 mm x 200 mm impact surface area) was added to the full body model.

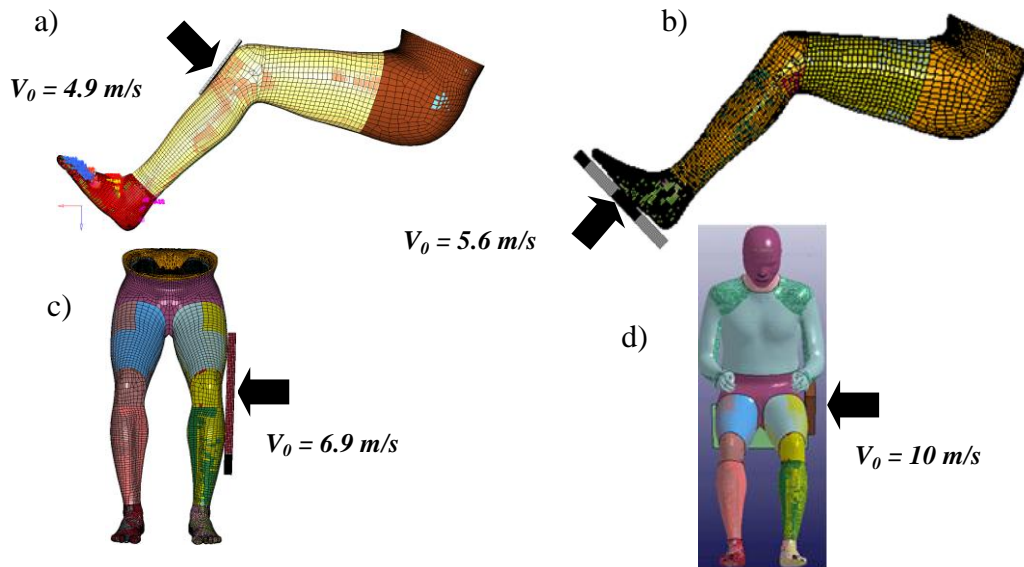


Figure 3. Stability check simulations a) frontal knee impact, b) lateral knee impact, c) axial foot impact, and d) lateral pelvic impact

Results and Discussion

The whole PLEX FE model has 285 distinct components which contain almost 626,000 elements (98.6 % of them defined as deformable). The only rigid parts were defined in the forefoot bones due to the low significance of these injuries in traffic accident trauma. The solids represent the majority of elements (73 %), followed by shells (26.5 %) and bars elements (0.5 %). To increase the computational efficiency, mass scaling was applied to the PLEX model. Thus, a mass scaling to $0.3 \mu\text{s}$ time step resulted in an insignificant mass increase of the model (around 0.3 %) and was used in all simulations. The stability of the PLEX model with $0.6 \mu\text{s}$ minimal time step was also checked.

The lower limb FE model showed good agreement with PMHS data in terms of the biomechanical response and injury prediction in all validations tests (Untaroiu et al. 2011). In the knee-thigh-hip (KTH) impact validation (FO-1) a pelvic acetabulum fracture pattern was predicted by the simulation (Fig. 4b), as it was observed in testing. The time history of the simulated impact force shows to be close to the upper bound of the test data, with a peak fracture force around 6 kN (Fig. 4c).

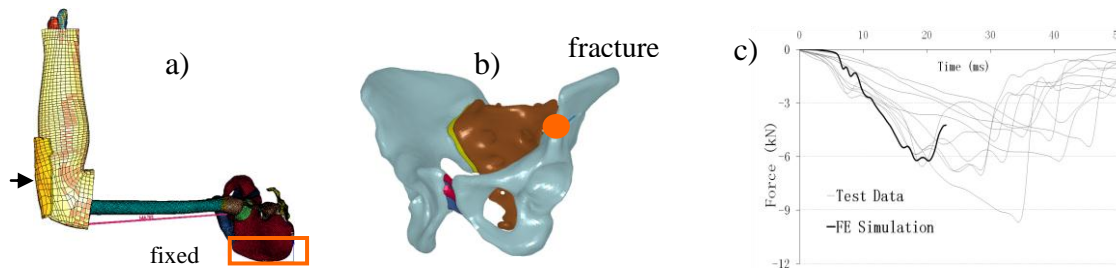


Figure 4. The validation of knee-thigh-hip model a) test setup b) injury prediction c) test data vs. computer results (Yue et al. 2011)

In the pedal impact validation (FO-11), the deformed shape of the foot-leg-thigh FE model with the pedal model at 30 msec is illustrated in Fig. 5a. The cross sectional forces, cross sectional moment, and the angular displacements were calculated during the simulation. These computational results were compared against experimental data to assess the moment-angle response of the foot and ankle FE model (Fig. 5c). In particular, the calculated moment and angle response at the ankle location shows good agreement with the average test curve-fit data provided by Rudd et al. (2004). In their tests, the measured moment and angle responses of the ankle joints of eighteen PMHS were used to establish an average response for comparison to the response of dummies and FE models (Rudd et al. 2004). Furthermore, the location and incidence of bony fracture or ligament failure were compared to injuries reported in the corresponding tests (Rudd et al. 2004) via autopsy and acoustic emission data. The computational model predicted failure of the posterior talotibial ligament at 30 msec, which corresponds to the maximum moment occurring in the ankle, followed by a medial malleolus fracture. These predicted failures correspond to the most common type of ligament injury and bony fracture reported by Rudd et al. (2004) (Fig. 5b).

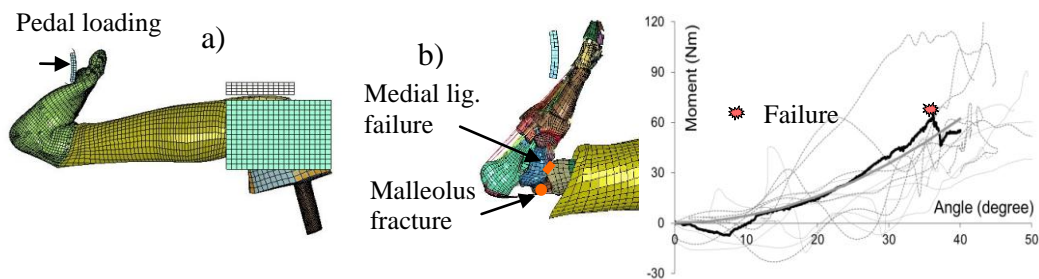


Figure 5. The validation of foot model under dorsiflexion loading a) test setup b) injury prediction c) test data vs. computer results (Shin et al. 2012)

To simulate the pelvic tolerance under lateral loading, dynamic and quasi-static loading were applied through a spherical ball fitted within each impact-side acetabulum (SO-2). Part of the coxal bone was fully constrained and a rigid plate with/without padding was placed against a metallic ball (3.68 kg). For quasi-static tests, the average displacement (magnitude) measured at six adjacent nodes on the pubic symphysis was compared to the experimental data. A good agreement between the experiments and model simulations are observed in terms of initial stiffness of the pelvic ring (Fig.6b).

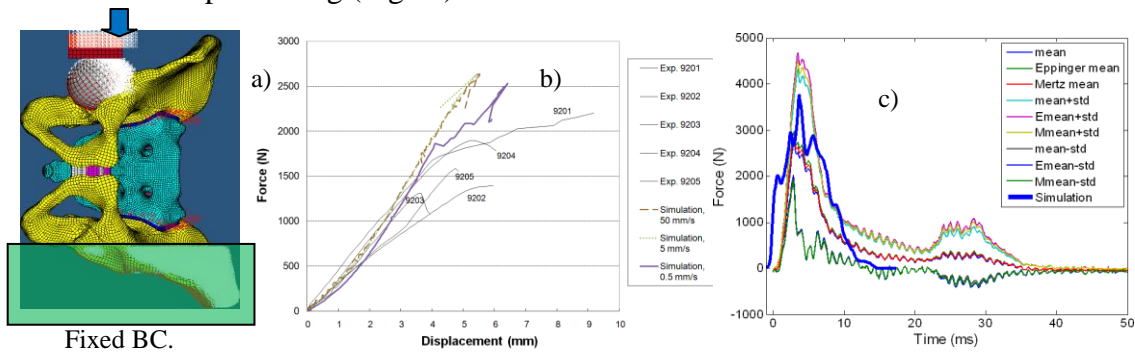


Figure 6. The validation of pelvis model under lateral impact loading (SO-2) a) test setup, test data vs. simulation data b) quasi-static conditions: load vs. displacement c) dynamic conditions: time histories of load

For the dynamic simulations (4 m/s initial velocity of loading plate), the impact force versus time response was compared to a corridor developed from experimental data from six male pelvises. The FE results are shown in blue, indicating that the force and displacement histories agree well with the corridor test data (Fig. 6c).

The PLEX model was found to be stable in all four model benchmarking simulations. In addition, the hourglass energy was under acceptable limits (e.g. 5% of total energy) in all simulations.

The model may be used in future for improving the current injury criteria of the pelvis and lower extremity (Untaroiu 2010) and the design of anthropometric test devices. Furthermore, the present pelvis and lower limb was coupled together with other body region FE models into a state-of-art human FE model to be used in the field of automotive safety (Fig. 3 d). The new human FE model will be used to better understand the injury mechanisms during vehicle crashes and develop advanced restraint systems.

Acknowledgements

The authors would like to acknowledge the Global Human Body Models Consortium, LLC (GHBMC) for supporting the development of the model.

References

1. Anderson AE, Peters CL, Tuttle BD, Weiss JA. (2005), Subject-specific finite element model of the pelvis: development, validation and sensitivity studies, *J Biomech Eng.* 2005 Jun; 127(3):364-73.
2. Balasubramanian S, Beillas P, Belwadi A, Hardy WN, Yang KH, King AI, Masuda M. (2004), Below Knee Impact Responses using Cadaveric Specimens, *Stapp Car Crash Journal*, 48: 71-88.
3. Beillas P, Begeman PC, Yang KH, King AI, Arnoux PJ, Kang HS, Kayvantash K, Brunet C, Cavallero C, Prasad P. (2001), Lower Limb: Advanced FE model and New Experimental Data, *Stapp Car Crash Journal*, 45: 469-494.
4. Bouquet, R., Ramet, M., Bermond, F., Caire, Y., Talantikite, Y., Robin, S., Voiglio, E. (1998) Pelvis human response to lateral impact. In: *Proceedings of the 16th International Technical Conference on the Enhanced Safety of Vehicles*, Windsor, ON, Canada, p. 1665-1686
5. Beason, D. P., Dakin, G. J., Lopez, R. R., Alonso, J. E., Bandak, F. A., and Eberhardt, A. W. (2003) Bone mineral density correlates with fracture load in experimental side impacts of the pelvis. *J. Biomech.*, 36(2), p. 219-227.
6. Chen, J., Siegler, S., Schneck, C.D. (1988) The Three-Dimensional Kinematics and Flexibility Characteristics of the Human Ankle and Subtalar Joints - Part II: Flexibility Characteristics. *Journal of Biomechanical Engineering*, vol. 110, pp. 374-385
7. Crandall, J.R., Bose, D., Forman, J., Untaroiu, C.D., Arregui-Dalmases, C., Shaw, C.G. and Kerrigan, J.R. (2011), Human surrogates for injury biomechanics research. *Clin. Anat.*, 24: 362–371.
8. Gayzik, F.S., Moreno, D., Greer, C., Wuertzer, S., Martin, R., and J.D. Stitzel (2011) Development of a Full Body CAD Dataset for Computational Modeling: A Multi-modality Approach, *Annals of Biomedical Engineering*, 39(10): 2568-2583.

9. Gordon, C.C., Churchill, T., Clauser, C.E., Bradtmiller, B., McConville, J.T., Tebbetts, I., Walker, R.A., 1989. 1988 anthropometric survey of US army personnel: methods and summary statistics. (NATICK/TR-89/044). US Army Natick Research, Development, and Engineering Center, Natick, MA.
10. Hewitt J, Guilak F, Glisson R, and TP Vail (2001), Regional Material Properties of the Human Hip Joint Capsule Ligaments, *Journal of Orthopaedic Research*, 19 (359-64).
11. Haug, E. (2001), H-Model Overview Description, *Proceedings of the Twenty-Ninth International Workshop on Human Subjects for Injury Biomechanics Research*.
12. Funk, J. R., Kerrigan, J. R. and Crandall, J. R., "Dynamic Bending Tolerance and Elastic-Plastic Material Properties of the Human Femur", 48th Annual Proceedings of AAAM, 2004.
13. Funk, J., Tournet, L., George, S., Crandall, J.R. (2000) The Role of Axial Loading in Malleolar Fractures. Paper 2000-01-0155, Society of Automotive Engineers.
14. Funk, J., Srinivasan, S., Crandall, J.R., Khaewpong, N., Eppinger, R., Jaffredo, A., Potier, P., Petit, P. (2002) The Effects of Axial Preload and Dorsiflexion on the Tolerance of the Ankle/Subtalar Joint to Dynamic Inversion and Eversion. *Proceedings of the 46th Stapp Car Crash Conference*, SAE paper 2002-22-0013.
15. Guillemot, H., Got, C., Besault, B., Lavaste, F., Robin, S., Le Coz, J. Y., and Lassau, J. (1998) Pelvic behavior in side collisions: static and dynamic tests on isolated pelvic bones. In: *Proceedings of the 16th ESV Conference*. Windsor, ON, Canada, p. 14412–14424.
16. Ivarsson BJ, Genovese D, Crandall JR, Bolton J, Untaroiu C, Bose D. (2009) The tolerance of the femoral shaft in combined axial compression and bending loading. *Stapp Car Crash Journal*; 53:251-290.
17. Keyak, J. H., Rossi, S. A., Jones, K. A. et al., "Prediction of femoral fracture load using automated finite element modeling", *Journal of Biomechanics*, 31:125-133, 1998
18. Kim YS, Choi HH, Cho YN, Park YJ, Lee JB, Yang KH, and AI King (2005), Numerical Investigations of Interactions between the Knee-Thigh-Hip Complex with Vehicle Interior Structures, *Stapp Car Crash Journal*, 49:85-115.
19. Kim, Y.H., Kim, J.E., Eberhardt, A.W., "A New Cortical Thickness Mapping Method with Application to an In-Vivo Finite Element Model, in review, *Computer Methods in Biomechanics and Biomedical Engineering*.
20. Kuppa, (1998) Axial Impact Characteristics of Dummy and Cadaver Lower Limbs, 16th ESV, Vol 2, pp 1608-1617.
21. Morgan, R.M., Eppinger, R., Marcus, J., and H. Nichols (1990) Human cadaver and hybrid III responses to axial impacts of the femur. *Proceedings of the International IRCOBI on Biomechanics Impacts*.
22. Robbins, D. H., Schneider, L. W. and Haffner, M., Seated Posture of Vehicle Occupants, *Stapp Car Crash Conference Proceedings*, # 831617, 1983.
23. Rudd, R., Crandall, J., Millington, S., Hurwitz, S. (2004) Injury Tolerance and Response of the Ankle Joint in Dynamic Dorsiflexion. *Stapp Car Crash Journal*, 48:1-26.
24. Silvestri, C. and M.H. Ray (2009) Development of a Finite Element Model of the Knee-thigh-hip of a 50 percentile male including ligaments and muscles, *International Journal of Crashworthiness*, 14 (2).
25. Shin, J., Yue, N., Untaroiu C.D. (2012) A Finite Element Model of the Foot and Ankle for Automotive Impact Applications, *Annals of Biomedical Engineering*, (under review).

26. Takahashi, Y., Kikuchi, Y., Konosu, A. and, H. Ishikawa (2000), Development and Validation of the Finite Element Model for the Human Lower Limb of Pedestrians, Stapp Car Crash Journal, 2000-01-SC22.
27. Untaroiu, C.D. (2005), Development and Validation of a Finite Element Model of Human Lower Limb, Ph.D dissertation, Department of Mechanical and Aerospace Engineering, University of Virginia, Charlottesville.
28. Untaroiu CD, Ivarsson BJ, Genovese D, Bose D, Crandall JR. Biomechanical injury response of leg subjected to dynamic combined axial and bending loading. *Biomedical Sciences Instrumentation* 2008; 44:141–146.
29. Untaroiu, C.D. (2010) “A numerical investigation of mid-femoral injury tolerance in axial compression and bending loading”, *International Journal of Crashworthiness*, (Impact factor 0.607, ISI citations: 2), 15(1):83-92.
30. Untaroiu, CD et al. (2011) *The Finite Element Model of the GHBM Pelvis and Lower Extremities (LS-Dyna Version)*, User Manual.
31. Wheeler L, Manning P, Owen C et al (2000). Biofidelity of dummy legs for use in legislative crash testing. *International Vehicle Safety 2000 Conference Transactions*, London, England, 2000, pp 183-200.
32. Yamada, H. (1970), *Strength of Biological Materials*, The Williams & Wilkins Company, Baltimore.
33. Yue N., Shin J., Untaroiu C.D., (2011) *A Numerical Investigation of Biomechanical and Injury Response of Occupant Lower Extremity during Automotive Crashes*, NHTSA Workshop.